



Tribological Performance of Gd-DLC and Eu-DLC Coatings in the Presence of Synthetic Oils Containing Ionic Liquid Additives

T. Omiya^{1,3} · M. Fontes^{1,2} · T. Vuchkov^{1,3} · S. Cruz^{1,3} · A. Cavaleiro^{1,3} · F. Ferreira^{1,3,4}

Received: 5 January 2023 / Accepted: 13 April 2023 / Published online: 30 April 2023
© The Author(s) 2023

Abstract

The lubrication of gadolinium-doped diamond-like carbon (Gd-DLC) and europium-doped diamond-like carbon (Eu-DLC) coatings with trihexyltetradecylphosphonium bis(2-ethylhexyl) phosphate ([P₆₆₆₁₄][DEHP]) ionic liquid (IL) as 1 wt% additive in polyalphaolefin (PAO) 8 was studied. The results of the friction tests under boundary lubrication conditions showed that Gd-DLC and Eu-DLC coatings in the presence of the IL exhibit a friction reduction, especially with the high atomic concentration of doped metal. Later, the surface observation after the long-term wear test indicated that Gd-DLC coatings have less abrasive wear and higher anti-wear properties compared to Eu-DLC coatings due to the enhanced formation of tribofilms derived from the phosphorus of the IL on the steel ball as the counter body. From these results, we have concluded that the friction reduction and the anti-wear property in the presence of the IL can be improved by changing the type and the concentration of the doped metals. This clearly shows that the novel lubrication system combining the Gd-DLC and Eu-DLC coatings with the IL allows for guiding future research and development.

✉ T. Omiya
omiya1130@gmail.com

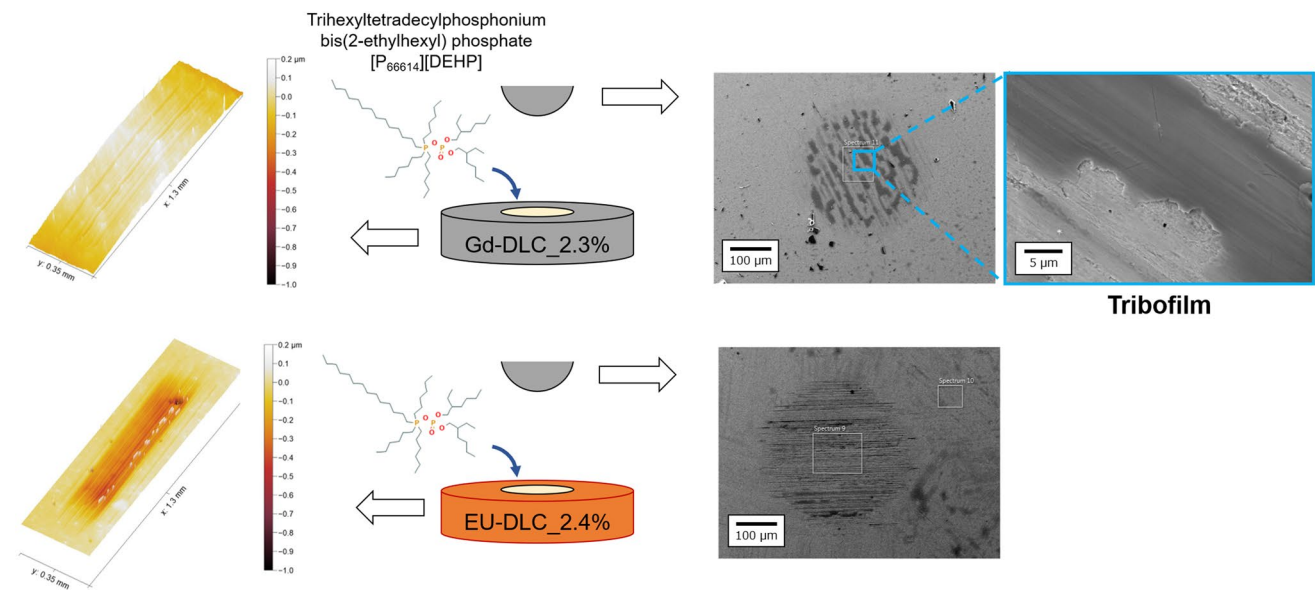
¹ Department of Mechanical Engineering, CEMMPRE Centre for Mechanical Engineering Materials and Processes, University of Coimbra, Rua Luís Reis Santos, 3030-788 Coimbra, Portugal

² Federal Institute of Education, Science and Technology of Sao Paulo, Rua Américo Ambrósio, Sertãozinho, São Paulo 14169-263, Brazil

³ Laboratory for Wear, Testing & Materials, Instituto Pedro Nunes, Rua Pedro Nunes, 3030-199 Coimbra, Portugal

⁴ Walker Department of Mechanical Engineering, The University of Texas at Austin, Austin, TX 78712, USA

Graphical abstract



Keywords Ionic liquid · Doped DLC · Boundary lubrication · Wear testing

1 Introduction

Climate change has been influencing the lubrication paradigm since energy consumption is directly linked to friction, especially in transportation systems [1]. Approximately 30% of energy consumption is due to transport vehicles, of which about one-third is lost due to friction and wear of transport vehicle components [2]. It is also known that friction, lubrication, and wear are the key points for the efficiency and lifetime of industrial machinery as well as vehicle components, thus impacting on national economies as indicated in several studies [3–5]. In addition to the high amount of CO₂ emitted by transportation systems, the consumption of mineral oils as lubricants is a serious environmental problem due to limited petroleum resources and the need to eliminate it from the environment. Therefore, significant efforts have been made worldwide to improve the energy efficiency and wear resistance of moving mechanical components.

To achieve these goals, several approaches have been taken, at the level of surface modification of mechanical components, along with the lubricant level to be less polluting. Diamond-like carbon (DLC) coatings have been used as coatings since they show excellent tribological performance and mechanical properties like high hardness, high resistance to wear, and low coefficient of friction (CoF) [6–8]. These exceptional properties make it possible to apply DLC, for example, in space tribology [9], photovoltaic technology [10], cutting tools [11], biomedical applications [12], or automotive engine components [13]. The

properties can be tuned by the chemical structure of DLC, sp²-, and sp³-bonded carbon atoms, which make it suitable for several industry fields, such as automotive, electronics, optics, aerospace, or even medical equipment. No matter the field of application, tribology performance of the mechanical components is an important issue to study. Owing to the increasing concern to reduce oil consumption in mechanical systems and, subsequently, the increased severity of contact conditions, many of these systems operate under boundary and starvation lubrication conditions [14–17]. Consequently, to achieve proper performance in such conditions, some interactions between coatings, lubricants are required for long-term, low wear, and friction operation. However, DLC coatings are known as "inert" coatings with low surface energy [18, 19], i.e., they do not react with various oil additives and/or by attracting polar groups of the additives and oil, which are the conventional mechanisms for lubricating steels and other metals [17]. Therefore, doping techniques have been usually used for synthesizing different types of DLC coatings to enhance the existing or impart new properties. Metals of non-carbide formers such as copper, silver, and aluminum [20–22], or metals of carbides formers such as chromium, titanium, tungsten, molybdenum, zirconium, and niobium [23–27], have been broadly researched as doping elements to decrease the high internal residual stress existing in as-grown DLC films and improve several properties, including adhesion to the substrate, thermal stability, corrosion resistance, and biocompatibility [28].

Also, although they are frequently mentioned as self-lubricating coatings, DLC thin films may have high specific wear rates when used under dry conditions. To increase its service life, a liquid lubricant can be employed [29]. As was mentioned before and according to Rübiger et al. [30], one of the main limitations of DLC is their low reactivity with currently used oil additives, which reduces the formation of sacrificial tribofilms from anti-wear additives (e.g., zinc dialkyl dithiophosphate). In the last three decades, several studies were published about the interaction between base oils (BOs), lubricant additives, and doped DLC coatings [31–37]; however, a general consensus has not been reached yet. In addition, as new additives are being synthesized, as ZrO₂-MoDTC hybrid nanoparticles or microgels [38, 39], to improve the energy efficiency of moving mechanical components, the lubrication mechanism, and performance of these new additives, when used in the presence of DLC films, are not yet established.

Among the various lubricant additives that have been studied in recent years, ionic liquids (ILs) have attracted significant interest due to their unique properties, such as high thermal stability, low flammability, low vapor pressure, and high tunability [40–46]. ILs are composed of organic compounds made of anions and cations. Phosphorus-containing ILs have shown particular promise in reducing friction and wear by forming a protective film on steel and aluminum surfaces under harsh contact conditions [47–49]. Qu et al. reported that trihexyltetradecylphosphonium bis(2-ethylhexyl) phosphate ([P₆₆₆₁₄][DEHP]), which is soluble in nonpolar solvents, reacts at steel/cast iron sliding interfaces to form surface layers suggested to consist of iron phosphate, especially at high temperatures [50–52]. More recently, Li et al. investigated the reactivity of [P₆₆₆₁₄][DEHP] on steel surfaces using in situ atomic force microscopy (AFM) [53]. The study provided evidence that under conditions leading to the removal of the native oxide layer from steel surfaces, phosphate anions adsorb onto metallic iron surfaces and lead to the formation of a densely packed boundary layer that reduces nanoscale friction.

Despite the relevance of these studies, only a few focus on the improvements achieved by DLCs when lubricated by ILs as a lubricant or oils that only use ILs with anti-wear additives. Gonzalez et al. studied the lubrication of coatings growth by physical vapor deposition (PVD) at high contact pressures, using a mixture of 1-butyl-1-methylpyrrolidinium tris(pentafluoroethyl)trifluorophosphate ([BMP][FAP]) and polyalphaolefins (PAO) 6 [54]. They found that the mixture with [BMP][FAP] showed a greater reduction in wear, values similar to those achieved when using zinc dialkyl dithiophosphate (ZDDP), as an additive. Recently, Arshad et al. reported that dimethyl phosphate thermally decomposes to phosphate, which interacts with tungsten-doped DLC surfaces as chemisorption to form phosphate-based tribofilms that facilitate shear and reduce friction [55].

To promote the reactivity of the DLC surface, the rare earth metals group was not much explored. Usually, lanthanide ions are in the trivalent oxidation state (Ln(III)) [56], which gives them a high affinity for ILs. This is confirmed by several studies on the extraction of rare earth metals from different media using ILs [57–59] or promoting luminescent properties to these ILs [60]. According to these indications, it is expected that the use of lanthanides can influence the tribolayer formed in tribological processes, where the anti-wear additives are ILs.

In this study, we want to understand the behavior of lanthanides as reactive elements on the surface of DLC coating in order to evaluate the tribological performance by using ILs. DLC coatings, deposited using High Power Impulse Magnetron Sputtering (HiPIMS), were doped with two different rare earth metals, gadolinium or europium, with the aim of evaluating their lubrication performance when sliding against steel in the presence of synthetic oil containing [P₆₆₆₁₄][DEHP]. The mechanical and tribological properties of gadolinium-doped diamond-like carbon (Gd-DLC) and europium-doped diamond-like carbon (Eu-DLC) coatings were investigated, comparing samples lubricated with ILs and BO, in order to show the effectiveness of the doping process on the lubrication performance of the ILs.

2 Test Materials and Methods

2.1 Materials

Steel (AISI D2, 25 mm diameter and 4 mm thick) was used as the substrate for the mechanical and tribological tests, and silicon [100] wafer, 20 × 20 mm, was used as the substrate for the chemical composition analysis of the coatings. Before mirror-polishing the steel substrates, using a diamond paste ($Ra \approx 0.1 \mu\text{m}$), the samples were tempered at 200 °C, achieving a hardness of around 60 HRC. Through consecutive ultrasonic baths, all substrates were cleaned in acetone and absolute ethanol for 15 min each. After cleaning and before introducing the samples inside the deposition chamber, the substrates were glued onto an aluminum substrate holder using silver glue.

2.2 Process and Coating Deposition

DLC coatings were deposited by the sputtering technique with a DOMS (Deep Oscillation Magnetron Sputtering) power supply (HiPIMS Cyprium™ plasma generator, Zpulsar Inc.). For all depositions, the substrate holder revolved at 23.5 rev/min around the chamber central axis, and the substrates were kept 80 mm distance to the carbon and chromium targets.

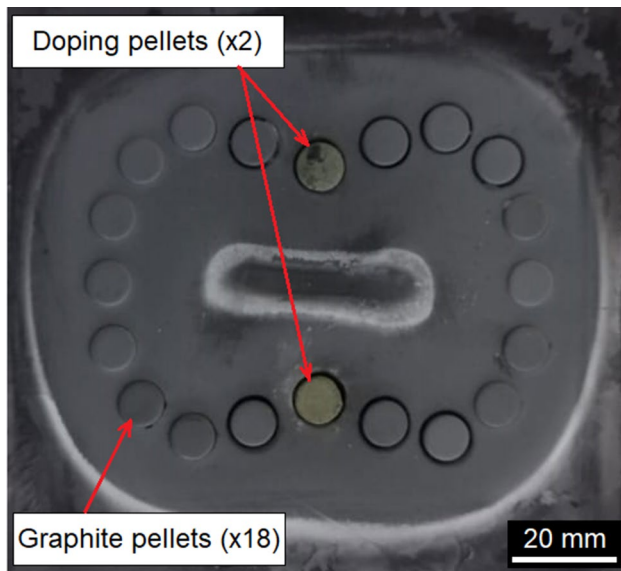


Fig. 1 Detail of the graphite target with the pellets

Table 1 Atomic concentration for each coating according to the number of doping pellets used

| Sample name | Number of doping pellets | Atomic % |
|-------------|--------------------------|---------------|
| Gd-DLC_1.7% | 1 | Gd: 1.7(±0.0) |
| Gd-DLC_2.3% | 2 | Gd: 2.3(±0.1) |
| Eu-DLC_1.7% | 1 | Eu: 1.7(±0.0) |
| Eu-DLC_2.4% | 2 | Eu: 2.4(±0.1) |

To deposit the DLC coatings and the Cr adhesion layer, a target with dimensions of 150 mm × 150 mm × 10 mm thick of pure graphite (purity 99.95%) and a target with the same dimension made of chromium (purity 99.99%) were used. Circular grooves of 10 mm diameter and 2 mm depth were machined in the graphite target to place the doping pellets (Gd or Eu pellets) during the deposition of the DLC coatings (Fig. 1). When using only one doping pellet, the other one was replaced by the graphite pellet. To obtain different atomic concentrations on the coatings, different pellets amounts were used. Table 1 shows information about the sample's identification and the atomic concentration of the doped element in each coating, analyzed by Rutherford Backscattering Spectrometry (RBS) and Elastic Recoil Detection (ERD).

A base pressure lower than 3×10^{-4} Pa was achieved inside the sputtering chamber by the combined use of a rotary and turbomolecular pump system. The chronological sequence of deposition process steps is described in the following topics:

1. Cleaning of the substrates and the targets to remove residues and oxides. For the carbon target, the cleaning was performed for 10 min, using a pressure of 0.4 Pa and average power of 600 W; the chromium target was cleaned for 60 min with a pressure set to 0.35 Pa and power of 250 W; the substrates were cleaned with a voltage of 345 V.
2. Deposition of two interlayers to improve the DLC coatings' adhesion to the substrates. First, a Cr layer was deposited by direct-current magnetron sputtering (DCMS) (deposition duration: 10 min; pressure: 0.3 Pa; DC substrate biasing: -60 V, chromium target power: 1200 W, pure Ar plasma). Afterward, a CrN layer was deposited with the Ar:N₂ gas flow ratio maintained at 1:3 by 7 min at 0.3 Pa. Both interlayers are around 400 nm thick.
3. Deposition of DLC coatings by HiPIMS for 57 min with a pressure of 0.4 Pa. The duration time of the micro-pulses was 6 μs, the micro-pulse period was 150 μs, and the duration time of the whole pulse was 1800 μs. The substrate voltage bias and the averaged power were equal to -80 V and 600 W, respectively.

2.3 Lubricants

PAO 8 was used as the base lubricant. Trihexyltetradecylphosphonium bis(2-ethylhexyl) phosphate [P₆₆₆₁₄][DEHP] was synthesized using the procedure outlined [42]. Briefly, trihexyl(tetradecyl)phosphonium bromide (95% purity, Strem chemicals) was mixed in methanol and treated with Amberlite IRN78 (99.9% purity, Alfa Aesar) to obtain trihexyl(tetradecyl)phosphonium hydroxide. The mixture was then filtered and treated with bis(2-ethylhexyl) hydrogen phosphate (TCI) and stirred for 3 days. Methanol and other volatiles were then removed at reduced pressure (~8 Torr) and temperature (~-50 °C). The water content of as-synthesized [P₆₆₆₁₄][DEHP] was 0.07% (700 ppm). The purity of as-synthesized [P₆₆₆₁₄][DEHP] was estimated by nuclear magnetic resonance (NMR) spectroscopy and found to be ≥ 92%. The lubricant of PAO 8 with 1 wt% of [P₆₆₆₁₄][DEHP] was prepared by mixing 1 g of [P₆₆₆₁₄][DEHP] in 99 g of PAO 8 using an analytical balance. The kinematic viscosity of the solution in the presence of 1 wt% of [P₆₆₆₁₄][DEHP] at 80 °C was 12.6 m²/s. The equations used to calculate the pressure viscosity coefficient, α , are given below. Equation 1 is the Walther (ASTM D341-77) equation and Eq. 2 is the Wu-Klaus-Duda equation, where A and m are specific material constants. The temperature T and the kinematic viscosity ν of the lubricant at 40 °C and 100 °C were substituted into Eq. (1), the simultaneous equations were solved and A and m were calculated. The pressure viscosity coefficient, α , was then calculated by substituting m into Eq. 2 [61].

Table 2 Frequency ranges and sliding speeds during friction testing

| Level | 1 | 2 | 3 | 4 | 5 | 6 | 7 | 8 | 9 |
|-------|-------|-------|-------|-------|-------|-------|-------|-------|-------|
| Hz | 5.00 | 4.50 | 4.00 | 3.50 | 3.00 | 2.75 | 2.50 | 2.25 | 2.0 |
| m/s | 0.150 | 0.135 | 0.120 | 0.105 | 0.090 | 0.083 | 0.075 | 0.068 | 0.060 |
| Level | 10 | 11 | 12 | 13 | 14 | 15 | 16 | 17 | – |
| Hz | 1.8 | 1.5 | 1.3 | 1.0 | 0.8 | 0.6 | 0.4 | 0.2 | – |
| m/s | 0.053 | 0.045 | 0.038 | 0.030 | 0.024 | 0.018 | 0.012 | 0.006 | – |

The pressure viscosity coefficient of the solution at 80 °C was 14.1 GPa.

$$\log_{10} \log_{10}(v + 0.7) = A - m \log_{10} T \quad (1)$$

$$\alpha = (0.1657 + 0.2332 \log_{10} v) \times m \times 10^{-8} \quad (2)$$

2.4 Characterization

Hardness and reduced Young's modulus were obtained by nano-indentation. The nano-indenter included a Berkovich diamond indenter. A maximum load of 10 mN (standard parameters in the CEMMPRE laboratory) was used to ensure an indentation depth that is less than 10% of the coating's thickness [62]. Sixteen different measurements were performed for each specimen to calculate the mean and the standard variation of the mechanical properties.

The scratch test, used to evaluate the adhesion of the coatings, was performed by an automatic scratch tester, model CSEM—REVETEST, fitted with a Rockwell “C” diamond-tipped indenter with a spherical tip diameter of 200 μm. The scratch test speed was set to 10 mm/min and was used with a normal load linearly increasing from 0 to 60 N. The loading rate was equal to 10 N/mm. Samples and indenter were cleaned with ethanol before testing. An optical microscope was used to quantify the adhesive properties of the coating. To check if these experiments provided reproducible and consistent results, the tests were repeated three times for each sample.

2.5 Tribological Tests

Tribological experiments were performed using a ball-on-disk tribometer (Rtec MFT-5000 tribometer) in reciprocating motion. In this study, “Stribeck-type” friction tests were carried out with low load. The load applied was 3 N, corresponding to a maximum Hertzian contact pressure of 0.66 GPa. Tests were carried out over the frequency range of 0.2-to-5.0 Hz over a 15 mm stroke length at 80 °C. The changes in frequency range and respective sliding speeds are given in Table 2. A new ball made of AISI 52,100 steel with a diameter of 10 mm was used in each test. Friction tests were carried out for 20 s at each frequency and the average

steady-state CoF values at each sliding speed was calculated. The average surface roughness (R_a) of the disk and ball is ~ 10 nm and ~ 100 nm, respectively. The lubrication regime was determined with the Hamrock-Dowson equation and λ values were found to be less than 1 in all the experimental conditions; thus, our system could be characterized by boundary lubrication [63].

A long-term wear test was also performed on a ball-on-disk type Rtec MFT-5000 tribometer sliding tribometer in reciprocating motion. The ball with a diameter of 10 mm was made of AISI 52,100 steel. The tests were carried out at 80 °C under a normal load of 100 N for a total sliding duration of 20 min in the presence of 1 wt% of [P₆₆₆₁₄][DEHP]. The ball reciprocated at 5 Hz with a stroke length of 1 mm, and each test was repeated at least three times. After tribological testing, balls and coatings were cleaned with n-heptane. Wear profiles were measured using a 3D white-light interferometer (Rtec Sigma). For a better comparison, the specific wear rate was calculated as: $W_r = V/(Fs)$, where V is the wear volume, F is the normal load, and s is the total sliding distance.

The chemical composition of the worn surface was obtained by an energy-dispersive X-ray spectrometer (EDS), (Oxford, X-MAXN) coupled to a field emission scanning electron microscope (FESEM) ZEISS MERLIN Compact/VP Compact. Three measurements were performed on the sample surface at a magnification of × 1000, with an acceleration voltage of 10 kV and a beam current of 300 pA.

3 Results and Discussion

3.1 Mechanical Characterization

The hardness and the reduced Young's modulus of the four coatings are shown in Fig. 2. The highest result was obtained for Gd-DLC with 1.7% atomic concentration with mean value around 23 GPa, while for Eu-DLC with 1.7% atomic concentration, the mean value was around 17 GPa. The reduced Young's modulus of the coatings ranges between 180 and 190 GPa. These hardness and Young's modulus values are comparable to pure DLC coatings produced by the authors using the same technique [64]. Therefore, despite the inclusion of dopant elements, the mechanical properties of the coatings were not affected.

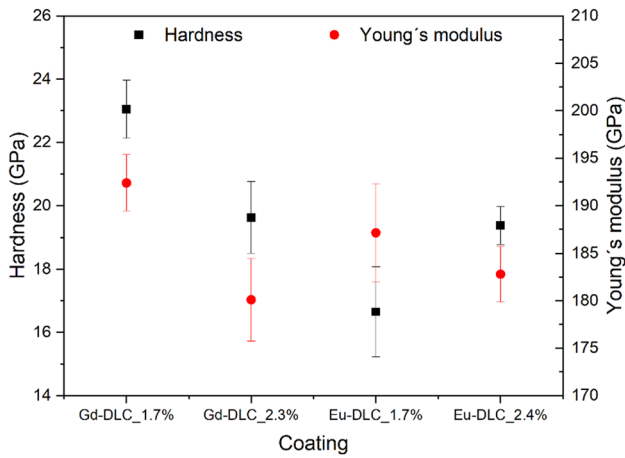


Fig. 2 Hardness and Young's modulus of the DLC coatings as a function of Gd and Eu atomic concentration

The morphological type, sp^2 or sp^3 hybridization, and the structural evaluation through density analysis can explain the differences got in hardness and reduced Young's modulus. Evaristo et al. [65], Ding et al. [64], and Kasiorowski et al. [66] reported that the high hardness obtained in DLC coatings can be achieved with a high amount of sp^3 hybridization in the amorphous carbon matrix, as well by the existing of a dense and compact structure on the DLC coating [67, 68]. According to Bai et al. [69], the decrease of sp^3/sp^2 ratio is responsible to decrease the DLC coatings hardness.

Figure 3 shows the optical micrographs of the scratch tracks produced on the DLC coatings, using a progressive load from 0 to 60 N. Dark edges associated with the material debris can be seen on the scratch tracks, indicating material removal without chipping. There was some chipping in the final phase of the test.

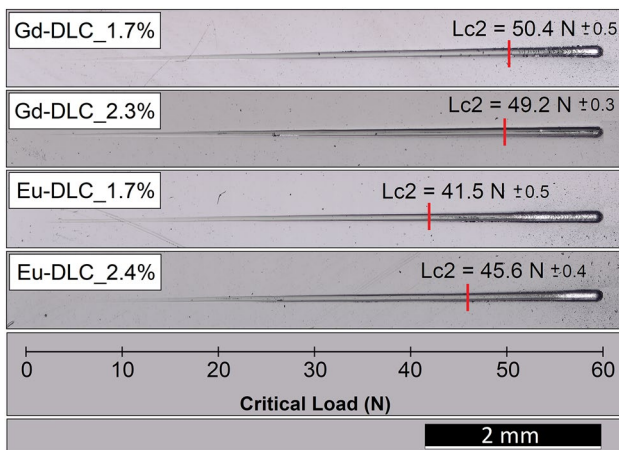


Fig. 3 Scratch tracks of DLC coatings

The critical load ($Lc2$), which was used to quantify the adhesion strength of the coatings, was defined as being the point where the coating chipping failure first appeared [70]. Coating removal in the scratch scar corresponds to the brighter areas in the optical image.

For all samples, a good adhesion of the coating to the substrate was obtained as chipping failure only occurred close to the final load. In agreement with the hardness and reduced Young's modulus results, the highest critical load value was obtained for Gd-DLC with 1.7 at.% Gd.

3.2 Friction Test

Friction tests were performed using PAO 8 as a base oil (BO) with and without 1 wt% [P_{66614}][DEHP]. Figure 4 shows that in the case of Gd- or Eu-doped DLC coatings, the presence of the IL in the BO lowers the CoF in the boundary lubrication condition. In addition, the results indicate that a higher atomic concentration of Gd and Eu facilitates the friction reduction effect, which was greater for Gd-DLC coating than for Eu-DLC coating. Although

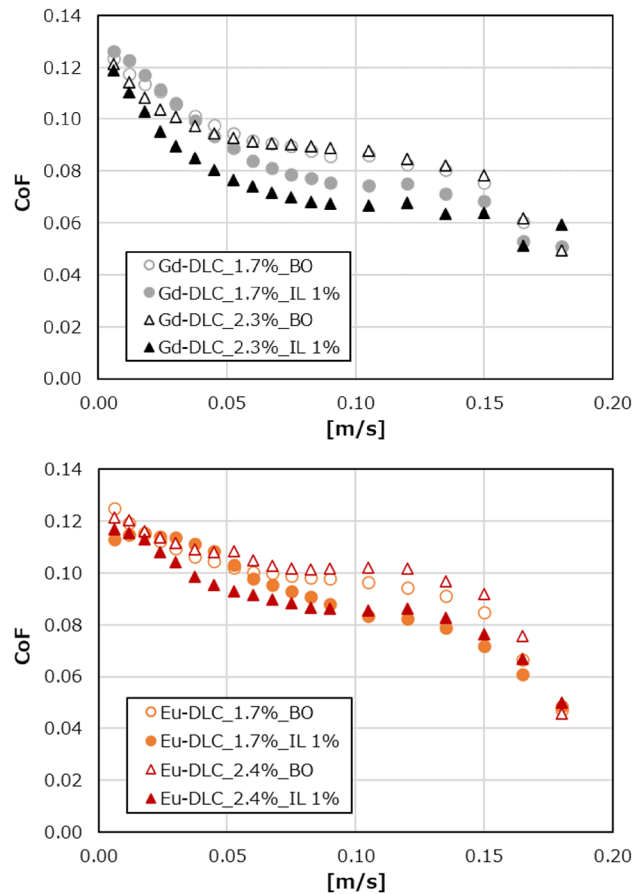


Fig. 4 CoF as a function of sliding speed for Gd-DLC and Eu-DLC coatings lubricated with PAO 8 with or without 1 wt% of [P_{66614}][DEHP]

the λ ratio calculations indicate a boundary lubrication condition for all velocity ranges, the CoF results were close for all samples near the low velocity (below 0.01 m/s), which reached an extreme boundary lubrication condition. The friction reduction effects of the IL especially for the Gd-DLC coatings were observed at velocities above 0.05 m/s, suggesting that there was an interaction between the IL and the coating.

3.3 Long-Term Wear Test

To evaluate the anti-wear property of the IL, a long-term wear test was conducted with both Gd-DLC and Eu-DLC coatings in the presence of 1 wt% of [P₆₆₆₁₄][DEHP] in PAO 8. The typical CoF evolution is shown in Fig. 5. It was observed that within the first 5 min of the test, a steady-state CoF was achieved, and no major changes were observed for the rest of the test. Figure 5b shows the average steady-state CoF values for the last one minute of test time in the three long-term wear tests. The standard deviation in Fig. 5b shows the error in the mean value of the CoF for the last one minute of the test in the triplicate test. Similar to the friction test results in the previous section, the Gd-DLC coatings had a higher friction reduction effect than the Eu-DLC coatings.

3.4 Surface Characterization

3.4.1 Wear Measurement on Coatings

To evaluate the anti-wear properties after the long-term wear test, 3D profilometry was used to measure the worn volume on both coatings and ball counter bodies. Figure 6 shows the wear track generated on Gd-DLC and Eu-DLC coatings lubricated with PAO 8 containing 1 wt% IL. The wear tracks of Gd-DLC coatings exhibit less wear when compared to the Eu-DLC coatings. In addition, from the appearance of the wear track, it can be seen that the wear decreased as the metal elements increased. The wear tracks contained scratch-like features in the direction of sliding, indicating that abrasive wear occurs. Among all coatings, the Eu-DLC_1.7% possesses the highest wear, potentially due to the lowest hardness of the coating.

The wear rate of each coating by measuring the wear volumes on the coatings is shown in Fig. 7. The standard deviations of the three tests are also shown in Fig. 7. Qu et al. have previously evaluated the anti-wear property of [P₆₆₆₁₄][DEHP] on steel/steel [44, 71]. Compared to their wear rates, it is clear that Gd-DLC and Eu-DLC coatings in this study significantly improved the wear rates. In general, it is said that the hardness of the coating has a significant effect on wear [72, 73]. However, although Fig. 2 reveals that Gd-DLC_2.3% and Eu-DLC_2.4% exhibit

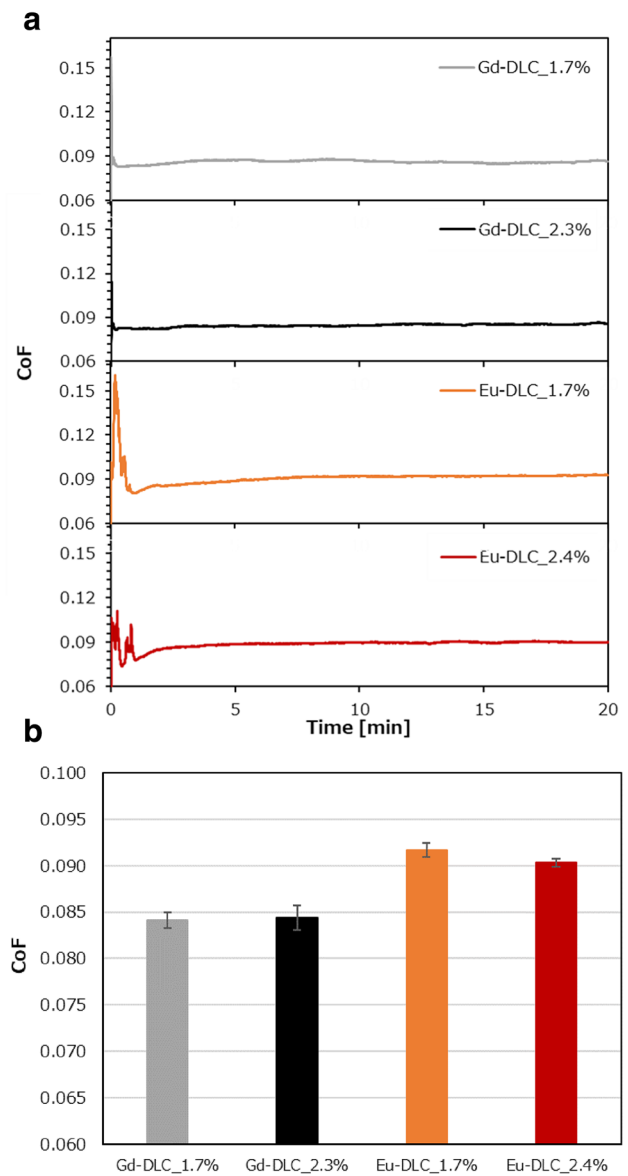


Fig. 5 a CoF during long-term wear tests of the DLC coatings and b CoF for last one minute of sliding

equal hardness, Fig. 7 surprisingly depicts a significant difference in the wear rates of both coatings, suggesting that Gd-DLC coatings have not only the friction reduction effect but also anti-wear property compared to Eu-DLC coatings. Furthermore, when comparing Gd-DLC coatings with each other, Gd-DLC_2.3% has a slightly lower hardness than Gd-DLC_1.7% in Fig. 2, while showing a lower wear rate in the presence of 1 wt% of [P₆₆₆₁₄][DEHP] compared to Gd-DLC_1.7%. The conclusion indicates that even if the hardness of the coating is lower, in the presence of the IL, the wear rate of the coatings can be improved by the type and amount of the doped metals. For a more detailed discussion of the anti-wear property

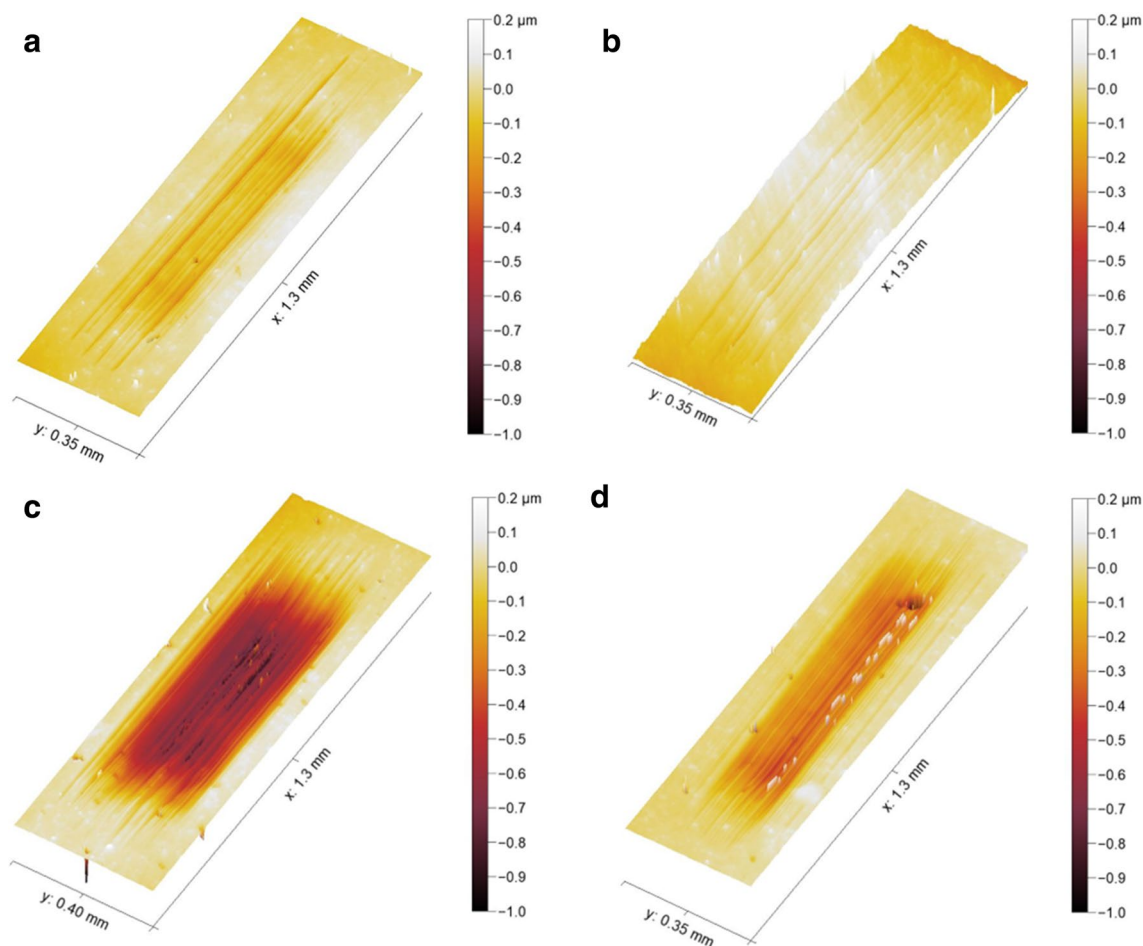


Fig. 6 a Wear track in the presence of 1 wt% of [P₆₆₆₁₄][DEHP] on Gd-DLC_1.7%; b Gd-DLC_2.3%; c Eu-DLC_1.7%; d Eu-DLC_2.4%

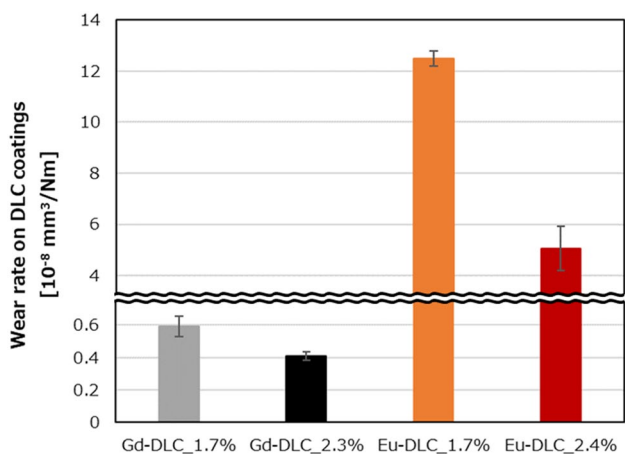


Fig. 7 Wear rate on Gd-DLC and Eu-DLC coatings in the presence of 1 wt% of [P₆₆₆₁₄][DEHP]

of the IL with the doped DLC coatings, the wear scars on the balls were evaluated.

3.4.2 Wear Measurement on Steel Balls

It can also be observed from Fig. 8 that the wear rate on the steel balls used in tests performed on Gd-DLC coatings was lower compared to the one of the worn area presents on Eu-DLC coatings. Compared to other literature that combines DLC coatings and IL [55, 74], the wear rates on steels from our study were lower or equal when tested with Gd-DLC coatings, inferring that a transfer layer like tribofilm was generated on steel balls that exhibit anti-wear properties similar to previous research works.

Figure 9a–d from SEM micrographs displays the worn region created on the steel balls using upon tribological testing. The SEM micrographs of the wear scars in Fig. 9 show that only in the case of the steel balls tested against

Gd-DLC coatings dark deposits could be detected. Figure 10 shows a magnified view of the dark deposits on the steel ball used against Gd-DLC_2.3% coating, displaying the formation of a tribofilm or transfer layer. On the other hand, a large amount of abrasive wear was observed on the steel

balls tested against Eu-DLC coatings. In addition, surface observations using SEM-EDS were performed to observe the composition of the transfer layer.

3.4.3 SEM-EDS Analysis

Surface observations using SEM-EDS were performed on the area indicated by the red frame on Gd-DLC_2.3% and Eu-DLC_2.4% used in the long-term wear test (Table 3). However, SEM-EDS couldn't detect phosphorus reliably on Gd-DLC_2.3% and Eu-DLC_2.4% coatings. Arshad et al. have successfully observed phosphate-based tribofilms on the tungsten DLC coatings using time-of-flight secondary-ion mass spectrometry (ToF-SIMS) [55]. Thus, it would be desirable to employ more surface-sensitive techniques like ToF-SIMS to confirm the effect of the IL on DLC coatings. The results of the elemental analysis of Eu-DLC_2.4% show that a large amount of chromium and nitrogen were detected, indicating that the CrN layer, which is an interlayer, got detected due to higher wear.

Similarly, the effect of the IL on the steel balls against the Gd-DLC_2.3% and Eu-DLC_2.4% coatings was evaluated by SEM-EDS. Table 4 also shows the results of the

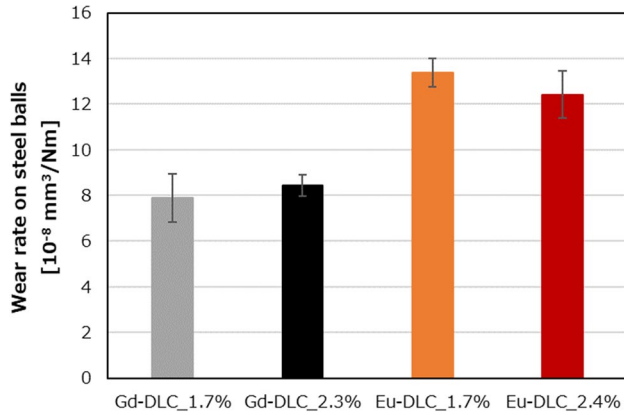


Fig. 8 Wear rate on steel balls for Gd-DLC and Eu-DLC coatings in the presence of 1 wt% of $[\text{P}_{66614}][\text{DEHP}]$

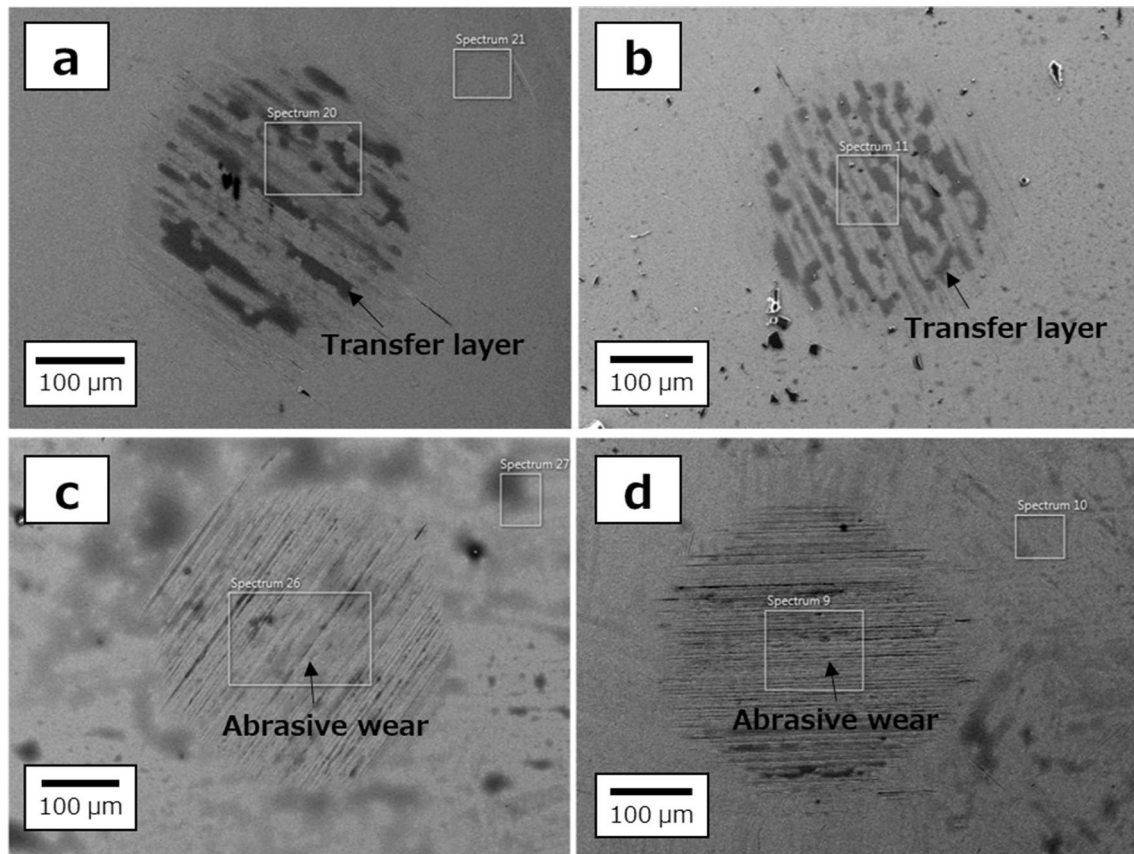


Fig. 9 SEM micrographs of the worn region on the 52,100 steel balls used for long-term wear tests **a** Wear behavior of steel balls tested with IL on Gd-DLC_1.7%; **b** on Gd-DLC_2.3%; **c** on Eu-DLC_1.7%; **d** on Eu-DLC_2.4%

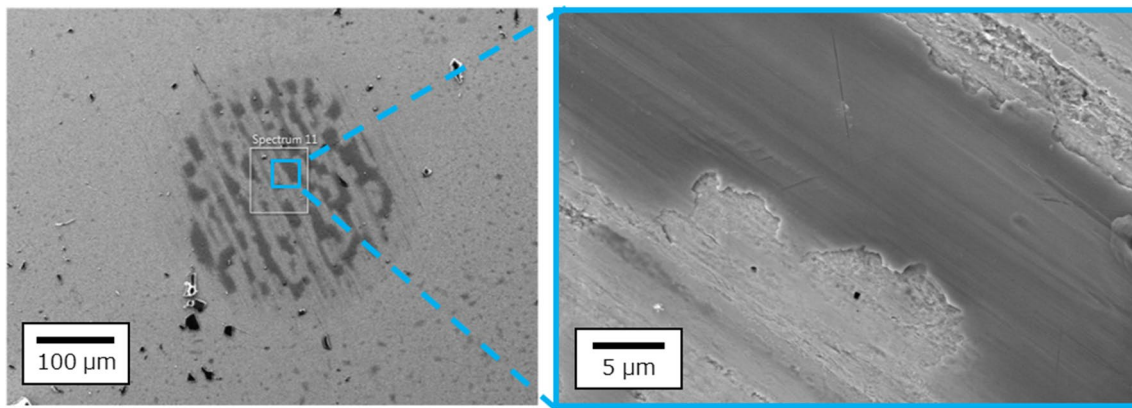


Fig. 10 Deposits on the steel ball against the Gd-DLC_2.3% coating

elemental analysis of the tribofilm on Gd-DLC_2.3%. It can be seen that the ball for Gd-DLC_2.3% has a higher atomic concentration of oxygen and phosphorus than the ball for Eu-DLC_2.4%. Barnhill et al. [44] revealed a tribofilm containing oxygen and phosphorus for the worn surfaces generated in the lubricants containing $[P_{66614}][DEHP]$. The deposits on the balls for Gd-DLC_2.3% contain more oxygen and phosphorus, indicating that the tribofilm was derived from the $[P_{66614}][DEHP]$. Although oxygen and phosphorus were observed in either Gd-DLC_1.7% or Gd-DLC_2.3% counter bodies, no such elements were observed in either Eu-DLC_1.7% or Eu-DLC_2.4% counter bodies, suggesting

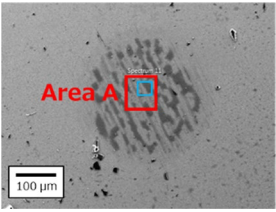
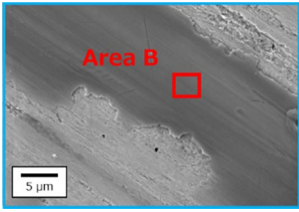
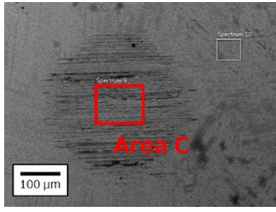
that no tribofilms were formed on the balls against Eu-DLC coatings.

Thus, the observation concludes that the Gd-DLC coating had a reduced wear rate due to the formation of a tribofilm on the balls. In the case of Eu-DLC coatings, it is not clear whether no tribofilm was formed or if tribofilm was formed and soon peeled off by wear debris. However, since no tribofilm was formed on the balls against Eu-DLC coatings, the wear rates were significantly elevated compared to the Gd-DLC coatings.

Table 3 Elemental Analysis on the Gd-DLC_2.3% and Eu-DLC_2.4% coatings using SEM-EDS

| | Gd-DLC_2.3% | | Eu-DLC_2.4% | |
|------------------------------------|------------------------|-----------------------|------------------------|-----------------------|
| SEM micrographs of the DLC coating | | | | |
| Element [at.%] | Area A Outside of wear | Area B Inside of wear | Area C Outside of wear | Area D Inside of wear |
| Cr | 2.5 | 2.7 | 2.0 | 9.0 |
| N | – | – | – | 3.6 |
| C | 92.0 | 91.8 | 91.7 | 82.3 |
| O | 2.5 | 2.4 | 3.8 | 3.2 |
| Gd | 1.7 | 1.7 | – | – |
| Eu | – | – | 1.6 | 1.4 |
| other | 1.3 | 1.4 | 0.9 | 0.5 |

Table 4 Elemental Analysis of the steel ball against the Gd-DLC_2.3% and Eu-DLC_2.4% coatings using SEM–EDS

| | Gd-DLC_2.3% | | Eu-DLC_2.4% |
|------------------------------|---|--|---|
| SEM micrographs of the balls |  |  |  |
| Element [at.%] | Area A Inside of wear | Area B Deposits on wear | Area C Inside of wear |
| O | 31.8 | 61.1 | 3.7 |
| P | 5.1 | 15.7 | 0.3 |
| Fe | 36.4 | 15.7 | 39.1 |
| C | 24.7 | 4.7 | 55.5 |
| Other | 2.0 | 2.8 | 4.4 |

4 Conclusion

This study investigates the interaction of 1 wt% of [P₆₆₆₁₄] [DEHP] on the surface of Gd-DLC and Eu-DLC coatings. From the results of the friction test, each DLC coating lubricated with PAO 8 and 1 wt% of the IL exhibited a low CoF compared to the BO reference under the boundary lubrication condition. In addition, higher the atomic concentration of doped metal increased the friction reduction effect, which was greater for Gd-DLC coatings than for Eu-DLC coatings. Later, the long-term wear test was also conducted on Gd-DLC and Eu-DLC coatings in the presence of 1 wt% of the IL to evaluate the anti-wear properties. Surprisingly, the wear rate results on the coating show that as the amount of metal doping increased, the wear rate on the coating decreased. The conclusion indicates that even if the hardness of the coating decreases with the doping of the DLC coating, the presence of the IL can improve the wear rate of the coatings by the type and amount of the doped metals. Furthermore, the surface observation using SEM–EDS revealed the formation of the tribofilm derived from the IL on Gd-DLC coatings, which played a significant role in wear reduction during the wear test. In the future, we will investigate further the DLC coating surface with techniques like ToF–SIMS to understand the interaction between the IL and the DLC coatings. However, the present work provides a correlation of physicochemical properties and tribological performance in a novel lubrication system combining the [P₆₆₆₁₄][DEHP] and doped DLC coatings with various metal atoms, such as Gd and Eu, which are expected to guide future research and development.

Acknowledgements This research was funded by FEDER funds through the program COMPETE—Programa Operacional Factores de Competitividade, by national funds through FCT—Fundação para a Ciência e a Tecnologia, under the project UIDB/00285/2020 and Lub-Energy (UTAP-EXPL/NPN/0046/2021), and by UT Austin Portugal research internship program 2022. The authors want to acknowledge Professor Filippo Mangolini for providing the ionic liquid and for his valuable result discussions.

Author contributions Takeru Omiya, Marcos Fontes, and Sandra Cruz wrote the main manuscript text. Also, Marcos Fontes prepared figures 1–3, and the rest of the figure was created by Takeru Omiya. All authors reviewed the manuscript.

Funding Open access funding provided by FCTIFCCN (b-on). Funding was provided by Fundação para a Ciência e a Tecnologia (UIDB/00285/2020). This work was supported by FEDER funds through the program COMPETE – Programa Operacional Factores de Competitividade, by national funds through FCT – Fundação para a Ciência e a Tecnologia, under the project UIDB/00285/2020 and Lub-Energy (UTAP-EXPL/NPN/0046/2021), and by UT Austin Portugal research internship program 2022.

Data Availability The data that support the findings of this study are available from the corresponding author, T. Omiya, upon reasonable request.

Declarations

Conflict of interest The authors have no competing interests.

Open Access This article is licensed under a Creative Commons Attribution 4.0 International License, which permits use, sharing, adaptation, distribution and reproduction in any medium or format, as long as you give appropriate credit to the original author(s) and the source, provide a link to the Creative Commons licence, and indicate if changes were made. The images or other third party material in this article are included in the article's Creative Commons licence, unless indicated otherwise in a credit line to the material. If material is not included in the article's Creative Commons licence and your intended use is not permitted by statutory regulation or exceeds the permitted use, you will need to obtain permission directly from the copyright holder. To view a copy of this licence, visit <http://creativecommons.org/licenses/by/4.0/>.

References

- Holmberg, K., Erdemir, A.: The impact of tribology on energy use and CO₂ emission globally and in combustion engine and electric cars. *Tribol. Int.* **135**, 389–396 (2019)
- Holmberg, K., Andersson, P., Erdemir, A.: Global energy consumption due to friction in passenger cars. *Tribol. Int.* **47**, 221–234 (2012)
- Jost, H.P.: Lubrication (tribology) education and research. A Report on the Present Position and Industry Needs, Department of Education and Science, HM Stationary Office, London, 4 (1966)
- Pinkus, O., Wilcock, D.F.: Strategy for energy conservation through tribology. Research Committee on Lubrication, Mechanical Technology Incorporated Tribology Dept, 174 (1977)
- Molgaard, J.: Economic losses due to friction and wear—research and development strategies. A Workshop Report, National Research Council Canada, Associate Committee on Tribology, 153 (1984)
- Zichao, L., Bin, S., Fanghong, S., Zhiming, Z., Songshou, G.: Diamond-coated tube drawing die optimization using finite element model simulation and response surface methodology. *Proc. Inst. Mech. Eng. B* **228**, 1432–1441 (2014)
- Santiago, J.A., Fernández-Martínez, I., Sánchez-López, J.C., Rojas, T.C., Wennberg, A., Bellido-González, V., et al.: Tribomechanical properties of hard Cr-doped DLC coatings deposited by low-frequency HiPIMS. *Surf. Coat. Technol.* **382**, 124899 (2020)
- Martins, P.S., Almeida Magalhães Júnior, P.A., Gonçalves Carneiro, J.R., Talibouya Ba, E.C., Vieira, V.F.: Study of Diamond-Like Carbon coating application on carbide substrate for cutting tools used in the drilling process of an Al–Si alloy at high cutting speeds. *Wear* **498–499**, 204326 (2022)
- Shi, B., Wu, Y.X., Liu, Y., Wang, L.M., Gao, J., Hei, H.J., et al.: A review on diamond-like carbon-based films for space tribology. *Mater. Sci. Technol.* **38**, 1151–1167 (2022)
- Lu, Y.M., Wang, S., Huang, G.J., Xi, L., Qin, G.H., Zhu, M.Z., et al.: Fabrication and applications of the optical diamond-like carbon films: a review. *J. Mater. Sci.* **57**, 3971–3992 (2022)
- Wang, L.J., Liu, Y., Chen, H., Wang, M.C.: Modification methods of diamond like carbon coating and the performance in machining applications: a review. *Coatings* **12**, 224 (2022)
- Peng, Y.L., Peng, J.H., Wang, Z.Y., Xiao, Y., Qiu, X.T.: Diamond-like carbon coatings in the biomedical field: properties, applications and future development. *Coatings* **12**, 1088 (2022)
- Kano, M.: Diamond-Like carbon coating applied to automotive engine components. *Tribol. Online* **9**, 135–142 (2014)
- Erdemir, A.: Review of engineered tribological interfaces for improved boundary lubrication. *Tribol. Int.* **38**, 249–256 (2005)
- Hsu, S.M., Gates, R.S.: Boundary lubricating films: formation and lubrication mechanism. *Tribol. Int.* **38**, 305–312 (2005)
- Neville, A., Morina, A., Haque, T., Voong, Q.: Compatibility between tribological surfaces and lubricant additives: how friction and wear reduction can be controlled by surface/lube synergies. *Tribol. Int.* **40**, 1680–1695 (2007)
- Velkavrh, I., Kalin, M., Vizintin, J.: The performance and mechanisms of DLC-coated surfaces in contact with steel in boundary-lubrication conditions: a review. *Stroj Vestn.-J. Mech. E* **54**, 189–206 (2008)
- Grischke, M., Hieke, A., Morgenweck, F., Dimigen, H.: Variation of the wettability of DLC-coatings by network modification using silicon and oxygen. *Diam. Relat. Mater.* **7**, 454–458 (1998)
- Sanchez-Lopez, J.C., Erdemir, A., Donnet, C., Rojas, T.C.: Friction-induced structural transformations of diamondlike carbon coatings under various atmospheres. *Surf. Coat. Technol.* **163**, 444–450 (2003)
- Balestra, R.M., Castro, A.M.G., Evaristo, M., Escudeiro, A., Mutafov, P., Polcar, T., et al.: Carbon-based coatings doped by copper: Tribological and mechanical behavior in olive oil lubrication. *Surf. Coat. Technol.* **205**, S79–S83 (2011)
- Manninen, N.K., Ribeiro, F., Escudeiro, A., Polcar, T., Carvalho, S., Cavaleiro, A.: Influence of Ag content on mechanical and tribological behavior of DLC coatings. *Surf. Coat. Technol.* **232**, 440–446 (2013)
- Bociaga, D., Komorowski, P., Batory, D., Szymanski, W., Olejnik, A., Jastrzebski, K., et al.: Silver-doped nanocomposite carbon coatings (Ag-DLC) for biomedical applications – Physicochemical and biological evaluation. *Appl. Surf. Sci.* **355**, 388–397 (2015)
- Voevodin, A.A., Capano, M.A., Laube, S.J.P., Donley, M.S., Zabinski, J.S.: Design of a Ti/TiC/DLC functionally gradient coating based on studies of structural transitions in Ti–C thin films. *Thin Solid Films* **298**, 107–115 (1997)
- Corbella, C., Vives, M., Pinyol, A., Bertran, E., Canal, C., Polo, M.C., et al.: Preparation of metal (W, Mo, Nb, Ti) containing a-C: H films by reactive magnetron sputtering. *Surf. Coat. Technol.* **177–178**, 409–414 (2004)
- Zhao, F., Li, H., Ji, L., Wang, Y., Zhou, H., Chen, J.: Ti-DLC films with superior friction performance. *Diam. Relat. Mater.* **19**, 342–349 (2010)
- Evaristo, M., Polcar, T., Cavaleiro, A.: Tribological behaviour of W-alloyed carbon-based coatings in dry and lubricated sliding contact. *Lubr. Sci.* **26**, 428–439 (2014)
- Ming, M.Y., Jiang, X., Piliptsov, D.G., Zhuang, Y., Rogachev, A.V., Rudenkov, A.S., et al.: Chromium-modified a-C films with advanced structural, mechanical and corrosive-resistant characteristics. *Appl. Surf. Sci.* **379**, 424–432 (2016)
- Wongpanya, P., Silawong, P., Photongkam, P.: Adhesion and corrosion of Al–N doped diamond-like carbon films synthesized by filtered cathodic vacuum arc deposition. *Ceram. Int.* **48**, 20743–20759 (2022)
- Zeng, Q.: Superlow friction and diffusion behaviors of a steel-related system in the presence of nano lubricant additive in PFPE oil. *J. Adhes. Sci. Technol.* **33**, 1001–1018 (2019)
- Rübig, B., Heim, D., Forsich, C., Dipolt, C., Mueller, T., Gebeshuber, A., et al.: Tribological behavior of thick DLC coatings under lubricated conditions. *Surf. Coat. Technol.* **314**, 13–17 (2017)
- Topolovec-Miklozic, K., Forbus, T.R., Lockwood, F., Spikes, H.: Asme: Behaviour of boundary lubricating additives on DLC coatings. In: Proceedings of the ASME/STLE International Joint Tribology Conference, pp. 141–143 (2007)
- Kalin, M., Velkavrh, I., Vizintin, J., Ožbolt, L.: Review of boundary lubrication mechanisms of DLC coatings used in mechanical applications. *Meccanica* **43**, 623–637 (2008)
- Velkavrh, I., Kalin, M.: Effect of base oil lubrication in comparison with non-lubricated sliding in diamond-like carbon contacts. *Tribol. Mater. Surf. Interfaces* **5**, 53–58 (2013)
- Kalin, M., Kogovšek, J., Remškar, M.: Nanoparticles as novel lubricating additives in a green, physically based lubrication technology for DLC coatings. *Wear* **303**, 480–485 (2013)
- Kosarieh, S., Morina, A., Lainé, E., Flemming, J., Neville, A.: The effect of MoDTC-type friction modifier on the wear performance of a hydrogenated DLC coating. *Wear* **302**, 890–898 (2013)
- Forsberg, P., Gustavsson, F., Renman, V., Hieke, A., Jacobson, S.: Performance of DLC coatings in heated commercial engine oils. *Wear* **304**, 211–222 (2013)
- Kalin, M., Velkavrh, I.: Non-conventional inverse-Stribeck-curve behaviour and other characteristics of DLC coatings in all lubrication regimes. *Wear* **297**, 911–918 (2013)

38. Sun, K.Q., Hu, Y.H., Dong, Y.H., Yao, L.L., Song, R.H., Xu, Y.F.: Tribological behavior of thermal- and pH-sensitive microgels under steel/CoCrMo alloy contacts. *Friction* **11**, 602–616 (2023)
39. Segu, D.Z., Chae, Y., Lee, S.-J., Kim, C.-L.: Synergistic influences of laser surface texturing and ZrO₂-MoDTC hybrid nano-fluids for enhanced tribological performance. *Tribol. Int.* **183**, 108377 (2023)
40. Suzuki, A., Shinka, Y., Masuko, M.: Tribological characteristics of imidazolium-based room temperature ionic liquids under high vacuum. *Tribol. Lett.* **27**, 307–313 (2007)
41. Bermudez, M.D., Jimenez, A.E., Sanes, J., Carrion, F.J.: Ionic liquids as advanced lubricant fluids. *Molecules* **14**, 2888–2908 (2009)
42. Somers, A.E., Khemchandani, B., Howlett, P.C., Sun, J., MacFarlane, D.R., Forsyth, M.: Ionic liquids as antiwear additives in base oils: influence of structure on miscibility and antiwear performance for steel on aluminum. *ACS Appl. Mater. Interfaces* **5**, 11544–11553 (2013)
43. Zhou, Y., Dyck, J., Graham, T.W., Luo, H., Leonard, D.N., Qu, J.: Ionic liquids composed of phosphonium cations and organophosphate, carboxylate, and sulfonate anions as lubricant antiwear additives. *Langmuir* **30**, 13301–13311 (2014)
44. Barnhill, W.C., Qu, J., Luo, H., Meyer, H.M., 3rd., Ma, C., Chi, M., et al.: Phosphonium-organophosphate ionic liquids as lubricant additives: effects of cation structure on physicochemical and tribological characteristics. *ACS Appl. Mater. Interfaces* **6**, 22585–22593 (2014)
45. Barnhill, W.C., Luo, H., Meyer, H.M., Ma, C., Chi, M., Papke, B.L., et al.: Tertiary and quaternary ammonium-phosphate ionic liquids as lubricant additives. *Tribol. Lett.* **63**, 22 (2016)
46. Zhou, Y., Qu, J.: Ionic liquids as lubricant additives: a review. *ACS Appl. Mater. Interfaces* **9**, 3209–3222 (2017)
47. Minami, I., Inada, T., Sasaki, R., Nanao, H.: Tribo-chemistry of phosphonium-derived ionic liquids. *Tribol. Lett.* **40**, 225–235 (2010)
48. Somers, A.E., Biddulph, S.M., Howlett, P.C., Sun, J., MacFarlane, D.R., Forsyth, M.: A comparison of phosphorus and fluorine containing IL lubricants for steel on aluminium. *Phys. Chem. Chem. Phys.* **14**, 8224–8231 (2012)
49. Sharma, V., Doerr, N., Aswath, P.B.: Chemical–mechanical properties of tribofilms and their relationship to ionic liquid chemistry. *RSC Adv.* **6**, 22341–22356 (2016)
50. Qu, J., Bansal, D.G., Yu, B., Howe, J.Y., Luo, H., Dai, S., et al.: Antiwear performance and mechanism of an oil-miscible ionic liquid as a lubricant additive. *ACS Appl. Mater. Interfaces* **4**, 997–1002 (2012)
51. Qu, J., Luo, H., Chi, M., Ma, C., Blau, P.J., Dai, S., et al.: Comparison of an oil-miscible ionic liquid and ZDDP as a lubricant anti-wear additive. *Tribol. Int.* **71**, 88–97 (2014)
52. Yu, B., Bansal, D.G., Qu, J., Sun, X., Luo, H., Dai, S., et al.: Oil-miscible and non-corrosive phosphonium-based ionic liquids as candidate lubricant additives. *Wear* **289**, 58–64 (2012)
53. Li, Z., Dolocan, A., Morales-Collazo, O., Sadowski, J.T., Celio, H., Chrostowski, R., et al.: Lubrication mechanism of phosphonium phosphate ionic liquid in nanoscale single-asperity sliding contacts. *Adv. Mater. Interfaces* **7**, 2000426 (2020)
54. González, R., Hernández Battez, A., Blanco, D., Viesca, J.L., Fernández-González, A.: Lubrication of TiN, CrN and DLC PVD Coatings with 1-Butyl-1-Methylpyrrolidinium tris(pentafluoroethyl) trifluorophosphate. *Tribol. Lett.* **40**, 269–277 (2010)
55. Arshad, M.S., Kovač, J., Cruz, S., Kalin, M.: Physicochemical and tribological characterizations of WDLC coatings and ionic-liquid lubricant additives: Potential candidates for low friction under boundary-lubrication conditions. *Tribol. Int.* **151**, 106482 (2020)
56. Valente, A.J.M., Burrows, H.D., Cruz, S.M.A., Pereira, R.F.P., Ribeiro, A.C.F., Lobo, V.M.M.: Aggregation and micellization of sodium dodecyl sulfate in the presence of Ce(III) at different temperatures: a conductometric study. *J. Colloid Interface Sci.* **323**, 141–145 (2008)
57. Turanov, A.N., Karandashev, V.K., Boltsova, M.: Solvent extraction of intra-lanthanides using a mixture of TBP and TODGA in ionic liquid. *Hydrometallurgy* **195**, 105367 (2020)
58. Mishra, B.B., Devi, N.: Application of bifunctional ionic liquids for extraction and separation of Eu³⁺ from chloride medium. *Trans. Nonferrous Met. Soc. China* **32**, 2061–2070 (2022)
59. Stoy, L., Xu, J.L., Kulkarni, Y., Huang, C.H.: Ionic liquid recovery of rare-earth elements from coal fly ash: process efficiency and sustainability evaluations. *ACS Sustain. Chem. Eng.* **10**, 11824–11834 (2022)
60. Rout, A., Kumar, S., Ramanathan, N.: Probing the coordination of europium(III) in a functionalized ionic liquid using luminescence spectroscopy. *J. Mol. Liq.* **323**, 115109 (2021)
61. Wu, C.S., Klaus, E.E., Duda, J.L.: Development of a method for the prediction of pressure-viscosity coefficients of lubricating oils based on free-volume theory. *J. Tribol.-Trans. Asme* **111**, 121–128 (1989)
62. Ferreira, F., Serra, R., Cavaleiro, A., Oliveira, J.: Diamond-like carbon coatings deposited by deep oscillation magnetron sputtering in Ar-Ne discharges. *Diam. Relat. Mater.* **98**, 107521 (2019)
63. Hamrock, B.J., Dowson, D.: Ball bearing lubrication (the elastohydrodynamics of elliptical contacts). *J. Lubr. Technol.* **104**, 279–281 (1981)
64. Ding, J.C., Chen, M., Mei, H., Jeong, S., Zheng, J., Yang, Y., et al.: Microstructure, mechanical, and wettability properties of Al-doped diamond-like films deposited using a hybrid deposition technique: Bias voltage effects. *Diam. Relat. Mater.* **123**, 108861 (2022)
65. Evaristo, M., Fernandes, F., Cavaleiro, A.: Room and high temperature tribological behaviour of W-DLC coatings produced by DCMS and hybrid DCMS-HiPIMS configuration. *Coatings* **10**, 319 (2020)
66. Kasiorowski, T., Lin, J., Soares, P., Lepienski, C.M., Neitzke, C.A., de Souza, G.B., et al.: Microstructural and tribological characterization of DLC coatings deposited by plasma enhanced techniques on steel substrates. *Surf. Coat. Technol.* **389**, 125615 (2020)
67. Aijaz, A., Ferreira, F., Oliveira, J., Kubart, T.: Mechanical properties of hydrogen free diamond-like carbon thin films deposited by high power impulse magnetron sputtering with Ne. *Coatings* **8**, 385 (2018)
68. Yetim, A.F., Kovacı, H., Kasapoğlu, A.E., Bozkurt, Y.B., Çelik, A.: Influences of Ti, Al and V metal doping on the structural, mechanical and tribological properties of DLC films. *Diam. Relat. Mater.* **120**, 108639 (2021)
69. Bai, M., Yang, L., Li, J., Luo, L., Sun, S., Inkson, B.: Mechanical and tribological properties of Si and W doped diamond like carbon (DLC) under dry reciprocating sliding conditions. *Wear* **484–485**, 204046 (2021)
70. Bull, S.J.: Failure modes in scratch adhesion testing. *Surf. Coat. Technol.* **50**, 25–32 (1991)
71. Zhou, Y., Weber, J., Viola, M.B., Qu, J.: Is more always better? Tribofilm evolution and tribological behavior impacted by the concentration of ZDDP, ionic liquid, and ZDDP-Ionic liquid combination. *Wear* **432–433**, 202951 (2019)
72. Bhushan, B.: Chemical, mechanical and tribological characterization of ultra-thin and hard amorphous carbon coatings as thin as 3.5 nm: recent developments. *Diam. Relat. Mater.* **8**, 1985–2015 (1999)

73. Neuville, S.: Antiwear material criteria. *JP J. Solids Struct.* **3**, 33–42 (2009)
74. Jia, Z., Xia, Y., Li, J., Pang, X., Shao, X.: Friction and wear behavior of diamond-like carbon coating on plasma nitrided mild steel under boundary lubrication. *Tribol. Int.* **43**, 474–482 (2010)

Publisher's Note Springer Nature remains neutral with regard to jurisdictional claims in published maps and institutional affiliations.